

# Suspension effect of BiPbSrCaCuO ceramics

Sang Heon Lee\*

Department of Electronics Information and Communication Engineering, Sun Moon University, Asan, Chung Nam 336-840, South Korea

Received 28 November 2003; received in revised form 10 December 2003; accepted 22 December 2003

Available online 6 May 2004

## Abstract

Magnetic flux measurements of a toroidal magnet revealed a concave shaped field distribution with a single minimum value and a null field along the axis of the torus at the point where the field was reversed. The non-linear magnetic field of the toroidal magnet perpendicular to the  $\text{Ag}_2\text{O}$ -doped superconducting disk sample with the trapped magnetic flux distorted the field line distribution. As a result, the interaction force between the magnet and sample exhibited regions of repulsive, null, attractive, null, and finally repulsive force. The asymmetrical concave shaped force pattern along the axis with two null force points indicates that the magnetic force exerted from the sample changed direction which resulted in the transition from repulsive force to attractive force at the null force point, and the force becomes repulsive again beyond the second null force point as the distance along the axis increases. The lateral stability of the suspended sample under the toroidal magnet is provided by the characteristics of the symmetrical nature of the field line with respect to the axis of the magnet. The magnetic moment of an undoped and 2%  $\text{Ag}_2\text{O}$ -doped sample was shown to be  $m = 0.043$  and  $0.06$  emu, respectively. The measured suspension force exerted from the doped sample agreed well with the suspension force calculated from magnetostatic force distribution.

© 2004 Published by Elsevier Ltd and Techna Group S.r.l.

**Keywords:** Magnetic flux; Magnetic suspension; Toroidal magnet;  $\text{Ag}_2\text{O}$

## 1. Introduction

The mechanical stability of a high temperature superconductor (HTS) held above or under a permanent magnet (PM) by levitating or suspending force determines the service ability of device such as magnetic bearings, energy storage flywheels and non-contact transport systems [1–3]. The levitation is accounted for the diamagnetic repulsive force with a gradient proportional to  $\text{d}B/\text{d}Z = J$  due to the Meissner effect in the HTS, where  $B$  is the flux density along the axial distance  $Z$  and  $J$  is the critical current density of the HTS sample [4,5]. Therefore, a large  $J$  is required to balance a large weight. The stable suspension of HTS under a PM is attributed to the flux pinning effect. The field cooling of the doped sample is preferred to enhance the flux pinning effect [6]. Lateral stability of the levitation/suspension system is another serious problem to counterbalance the lateral displacement, especially for transportation systems. A bowl shaped superconductor over which the PM floats is considered to provide a gravitational minimum value that leads to lateral stability [7].

The present work focuses on the suspension of field cooled BiPbSrCaCuO high  $T_c$  superconductor of 2%  $\text{Ag}_2\text{O}$ -doped samples under a toroidal permanent magnet. This measured suspension is compared with computer simulation of the magnetic field. The levitation is accounted for the diamagnetic repulsive force with a gradient proportional to  $\text{d}B/\text{d}Z = J$  due to the Meissner effect in the HTS, where  $B$  is the flux density along the axial distance  $Z$  and  $J$  is the critical current density of the HTS sample [4,5]. Therefore, a large  $J$  is required to balance a large weight. The stable suspension of HTS under a PM is attributed to the flux pinning effect. The field cooling of the doped sample is preferred to enhance the flux pinning effect [6]. Lateral stability of the levitation/suspension system is another serious problem to counterbalance the lateral displacement, especially for transportation systems. A bowl shaped superconductor over which the PM floats is considered to provide a gravitational minimum value that leads to lateral stability [7]. The present work focuses on the suspension of field cooled BiPbSrCaCuO high  $T_c$  superconductor of 2%  $\text{Ag}_2\text{O}$ -doped samples under a toroidal permanent magnet. This measured suspension is compared with computer simulation of the magnetic field.

\* Tel.: +82-41-530-2357; fax: +82-41-530-2910.  
E-mail address: shlee@sunmoon.ac.kr (S.H. Lee).

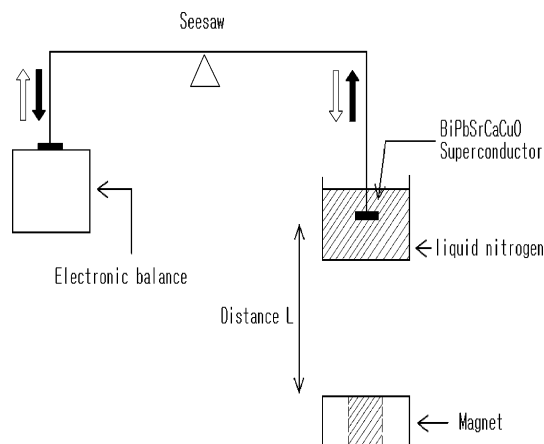


Fig. 1. Experimental setup of the force tester.

## 2. Experimental

The sample was made by the conventional solid state method using  $\text{Bi}_2\text{O}_3$ ,  $\text{PbO}$ ,  $\text{SrCO}_3$ ,  $\text{CaCO}_3$  and  $\text{CuO}$  powders of 99.9% purity. The molar ratio of the starting materials was 1.84:0.34:1.91:2.03:3.06, respectively, for Bi:Pb:Sr:Ca:Cu. The powder mixture was calcined in an alumina crucible at  $810^\circ\text{C}$  for 86.4 kS h in air. After grinding the calcined cakes, the precursor powder was mixed with  $\text{Ag}_2\text{O}$  powder of 99.9% purity. The powder mixtures were pressed into pellets under  $300\text{ kg/cm}^2$ , followed by sintering at  $830\text{--}850^\circ\text{C}$  for various time periods up to 432 kS. The pellet with a diameter of 8 mm and thickness of 1 mm weighed 0.3 g. The magnetic suspension of  $\text{BiPbSrCaCuO}$  (2223) superconductor beneath a toroidal permanent magnet was examined by means of a magneto-balancing at 77 K. The toroidal magnet used in this study was a samarium cobalt rare earth, NEOMAX,  $B = 0.15\text{ T}$ . The distribution of magnetic flux density along the axial direction was measured by using a gaussmeter, LakeShore Inc.

Forces were measured in a force tester consisting of a SmCo magnet and independent superconductor mounted on a pivoted frame, see Fig. 1. Magneto-balancing apparatus for the magnetic force measurement is illustrated schematically in Fig. 1. The sample was kept at 77 K at the bottom of the sample holder containing liquid nitrogen.

The sample holder was driven vertically so that the sample can move up and down through the magnet. Changes in the magnetic force, with the distance between the magnet and the sample, were thus measured.

## 3. Result and discussion

The magnetic field along the axis of the torus was calculated using the Poisson/Superfish code [8] for the toroidal magnet of 46 mm o.d., 12 mm i.d. and 10 mm thickness in the cylindrical coordinates ( $r$ ,  $\theta$ ,  $dz$ ). Dirichlet and Neumann boundary conditions were used to calculate the mag-

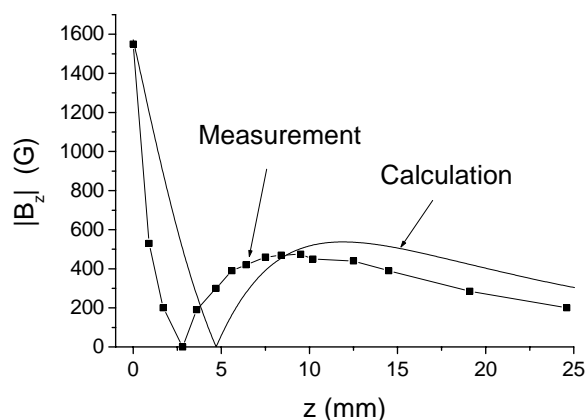


Fig. 2. Magnetic field strength along the symmetric axis by measurement and Poisson code calculation.

netic field for the boundaries parallel and perpendicular to the symmetry axis, respectively. The calculation boundaries were set to be sufficiently large value compared with the magnet size, and the magnetisation of toroidal magnet was assumed to be a constant along the axis direction. Magnetic field calculation was carried out with +1 and -1 stat-ampere of the surface current at  $r = 6$  and 23 mm surface, respectively, and the field strength at the magnet surface was set to be 0.15 T. The calculated magnetic field along the axis at the radial center showed a single asymmetric concave shaped distribution on each side of the magnet ( $Z > 0$  and  $Z < 0$ ) with a null field at 4.8 mm, where the field vector was reversed.

The calculated and measured strengths along the symmetric axis at  $r = 0$  are plotted in Fig. 2. One can see that the general patterns agree reasonably, except for the position of the null field. This may be attributed to the assumption of a constant magnetization in the axial direction we made in the calculation.

Fig. 3 shows the calculated the magnetic field line distribution around the toroidal magnet, which is consistent with the field distribution revealed by ferromagnetic particles above the toroidal magnet shown in Fig. 4. If the magnetic moment,  $m$ , of the HTS is assumed to be proportional to  $-B \cdot Z$ , the interacting magnetic force exerted on the HTS in the magnetic field  $B$  is given as  $F = m (dB/dZ)$ . Along the symmetric axis at  $r = 0$ ,  $F \propto B \cdot Z (dB/dZ)$ .

The interaction force between a 2%  $\text{Ag}_2\text{O}$ -doped HTS sample and a toroidal magnet is calculated and compared with the measured force by using an electronic balance along the symmetrical axis of the toroidal magnet as a function of axial distance, see Fig. 5. The presence of a HTS sample perpendicular to the non-linear magnetic field of a toroidal magnet distorts the original field lines distribution. As a result, the interaction force between the magnet and the sample exhibits a sort of concave shape consisting of the regions of repulsive force ( $Z < 4.8\text{ mm}$ ), attractive force ( $4.8 < Z < 11.8\text{ mm}$ ), null force ( $Z = 4.8$  and  $11.8\text{ mm}$ ) and repulsive force ( $Z > 11.8\text{ mm}$ ).

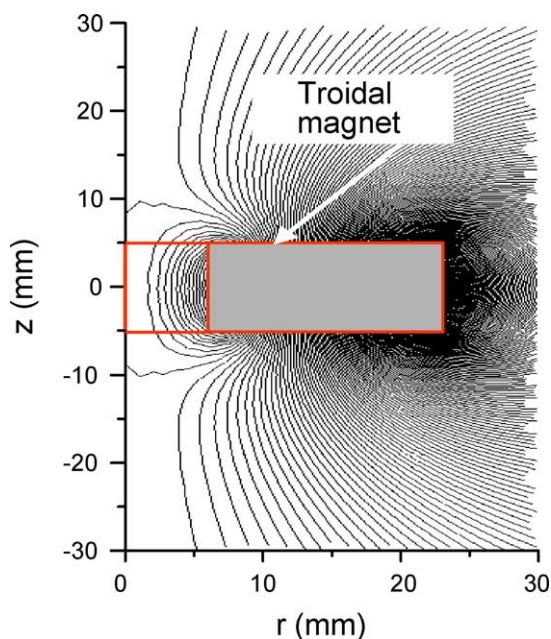


Fig. 3. Magnetic field lines by Poisson code calculation.

The results in Fig. 5 indicate that the force exerted on the HTS sample changes the direction with respect to the null force points along the  $Z$ -axis. The repulsive force in the repulsive force region along  $+Z$  direction balances the weight acting in the  $-Z$  direction, resulting in the stable levitation above a toroidal magnet. Similarly, by the symmetry with

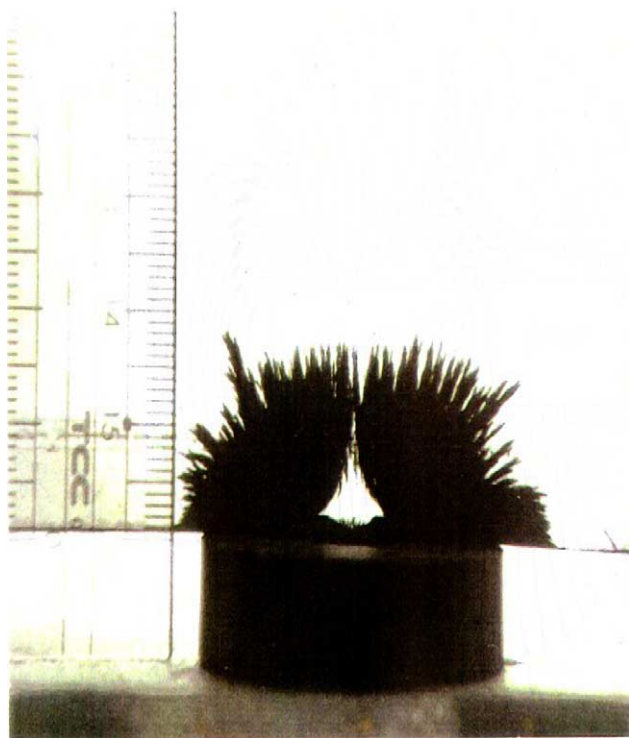


Fig. 4. Field distribution above the toroidal magnet revealed by ferromagnetic particles.

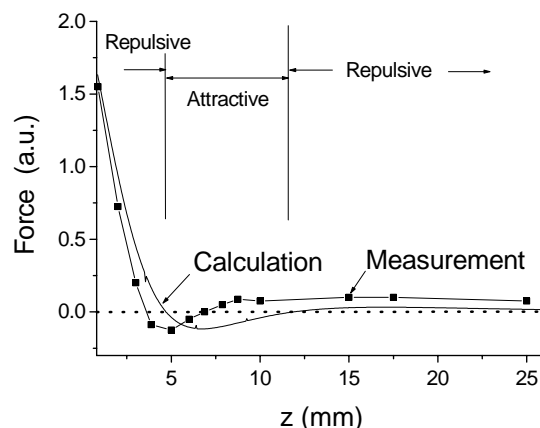


Fig. 5. Magnetic force exerted from the HTS sample in the non-linear magnetic field of the toroidal magnet.

respect to  $Z = 0$  plane, the suspension of the HTS sample occurs in the attractive region by balancing the weight. The asymmetric concave shaped magnetic force forms a vertical conical shaped magnetic wall around a levitated/suspended HTS sample, as demonstrated with a bowl shaped Type 1 superconductor lead providing a gravitational minimum value of the leading lateral stability [7]. Thus, the lateral stability of the levitated/suspended HTS sample above/beneath a toroidal magnet is achieved by the characteristics of the asymmetric nature of the magnetic force with respect to the axis of magnet.

The levitation was observed for both the undoped and doped samples at 77 K, however, the suspension occurred only for the 2%  $\text{Ag}_2\text{O}$ -doped and field cooled sample. The doped sample levitated at 3 mm above and suspended at 2 mm beneath the toroidal magnet, indicating the greater attractive force exerted on the sample. However, the difference between the measured and calculated distances of levitation/suspension may be caused by the assumptions of constant magnetization of the permanent magnet along the symmetric axis and  $m = -B \cdot Z$ . The suspension force of 1.21 mN measured by the electronic balance at the equilibrium for the 2%  $\text{Ag}_2\text{O}$ -doped of the field cooled condition agrees well with the suspension force calculated from the magnetostatic force curve in Fig. 5. The magnetic moment of the HTS calculated from the magnetization hysteresis was shown to be 0.043 emu for the undoped sample and 0.06 emu for the 2%  $\text{Ag}_2\text{O}$ -doped sample.

#### 4. Conclusions

The present work suggests that the successive regions of repulsive force, null force, attractive force, null force and repulsive force were produced along the axis of the toroidal magnet on both the top and bottom surfaces as a result of interaction between the HTS and the non-linear magnetic field of toroidal magnet. The resulting asymmetric concave

shaped magnetostatic force forms a magnetic wall around levitated/suspended sample, and also provides a gravitational minimum value at the equilibrium, thus the improved stability of magnetic bearing systems is expected. The suspension was observed only for the 2% Ag<sub>2</sub>O-doped sample and held the cooled sample which is attributed to the enhanced flux pinning effect due to the field cooled condition. This research was supported by a grant from Center for Applied Superconductivity Technology of the 21st Century Frontier R&D Program funded by the Ministry of Science and Technology, Republic of Korea.

## References

- [1] S. Sivrioglu, K. Nomori, Active permanent magnet support for a superconducting magnetic-bearing flywheel rotor, *IEEE Trans. Appl. Supercond.* 10 (4) (2000) 1673–1677.
- [2] M. Komori, K. Fukuda, A. Hirashima, A prototype magnetically levitated stepping motor using high  $T_c$  bulk superconductors, *IEEE Trans. Appl. Supercond.* 10 (2) (2000) 1626–1630.
- [3] K. Nagashima, Y. Iwasa, K. Sawa, M. Murakami, Controlled levitation of bulk superconductors, *IEEE Trans. Appl. Supercond.* 10 (3) (2000) 1642–1648.
- [4] M. Murakami, T. Oyama, H. Fujimoto, T. Taguchi, S. Gotoh, Y. Shiohara, N. Koshizuka, S. Tanaka, Large levitation force due to flux pinning in YBaCuO superconductors fabricated by melt–powder–melt–growth process, *Jpn. J. Appl. Phys.* 29 (11) (1990) L1991–L1994.
- [5] W. Henning, D. Parks, R. Weinstein, R.P. Sanhi, Enhanced levitation forces with field cooled YBa<sub>2</sub>Cu<sub>3</sub>O<sub>7- $\delta$</sub> , *Appl. Phys. Lett.* 72 (23) (1998) 3059–3061.
- [6] P.N. Peters, R.C. Sick, E.W. Urban, C.Y. Huang, M.K. Wu, Observation of enhanced properties in samples of silver oxide doped YBa<sub>2</sub>Cu<sub>3</sub>O<sub>x</sub>, *Appl. Phys. Lett.* 52 (24) (1988) 2066–2067.
- [7] F. Hellman, E.M. Gyorgy, D.W. Johnson Jr., H.M. O'Bryan, R.C. Sherwood, Levitation of a magnet over a flat type superconductor, *J. Appl. Phys.* 63 (2) (1988) 447–450.
- [8] J.H. Billen, L.M. Young, Poisson Superfish, Los Alamos National Laboratory Report, LA–UR–96–1834, 1997, pp. 253–262.